Impact of low order rationals in the enhanced confinement by pellet injection in TJ-II

L. García[1], B.A. Carreras[1], B.Ph. van Milligen[2], I. García-Cortés[2], K.J. McCarthy[2] and TJ-II team

[1] *Universidad Carlos III de Madrid, 28911 Leganés, Madrid, Spain*

[2] *Laboratorio Nacional de Fusión, CIEMAT, 28040 Madrid, Spain*

Introduction

An increase in confinement time associated with the injection of pellets has been observed in TJ-II [1, 2] and other devices. By means of a simple MHD model, we studied the modification of turbulent transport by the injection of pellets in TJ-II and how this modification affects the particle confinement time [3]. The analysis of the results showed the relationship of the confinement improvement with the evolution of the shear flow due to turbulence, especially near low order rational surfaces.

In a recent work [4], it was shown that confinement and L-H transitions of TJ-II are influenced by the modification of the rotational transform profile due to the plasma current. A confinement enhancement occurs when a low-order rational surface penetrates the plasma from the edge due to the modification of the rotational transform by the current. Both the confinement enhancement and the modification of the rotational transform are more pronounced in shots with pellets.

Here we explore the effect of current modification by pellet injection on turbulent transport. We choose the configuration 100_48_65 for the study since the low-order rational surface $n/m = 5/3$ is close to the plasma edge for this configuration. The pellet is modeled simply by adding a density source, as explained in Ref. [3]. Once the pellet is injected, we modify the rotational transform profile to simulate the effect of currents in the plasma, both externally induced and by the injection of the pellet. The mechanism for the confinement enhancement is the coupling of the $5/3$ and $8/5$ modes, which creates more internal barriers and reinforces the edge barrier.

Model and results

TJ-II is four-period stellarator of the heliac type with a major radius $R_0 = 1.5$ m, a minor radius $a \leq 0.22$ m and magnetic field strength at the torus axis $B_0 \leq 1.1$ T. Turbulence calculations are performed using an MHD turbulence model based on the reduced MHD equations. In this simple cylindrical model, interchange modes are the dominant instability. Since we do not model the three-dimensional magnetic geometry of the TJ-II stellarator, the calculations are not an accurate simulation of the TJ-II results yet have been very helpful in interpreting the experimental results, at least in a qualitative sense. Details of the model equations and parameter choices are given in Ref. [5]. The parameters of the model correspond to $n_{e0} = 3 \times 10^{19}\,\mathrm{m}^{-3}$, $T_{e0} = 0.3$ keV and $B_0 = 1.1$ T.

In the initial phase of the nonlinear calculation, the rotational transform profile corresponds to the currentless configuration 100_44_64, until a steady turbulent state is reached. The pellet is modeled by just adding a density source [3] for a very short time. Once the pellet is injected, we modify the rotational transform profile to simulate the effect of currents in the plasma, both externally induced and by the injection of the pellet.

Some of the rotational transform profiles used in the simulations are shown in figure 1. The shaded region corresponds to an artificial extension of the plasma to avoid numerical problems at $r = a$. The rotational transform is modified in three ways:

a) rescaling r in the rotational transform profile expression,

b) shifting the entire profile,

4) using a simplified model of the current [4].

In the experiments with pellets, the generated current shifts the 5/3 rational surface inward while maintaining the 8/5 rational in the plasma.

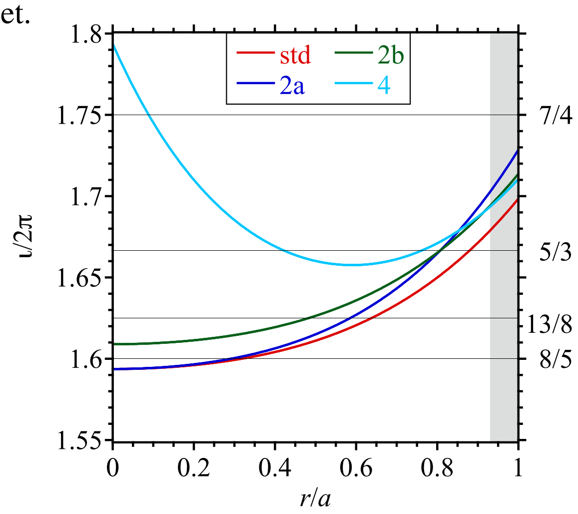

Figure 1: Rotational transform profiles of some cases. std denotes the standard (currentless) profile.

The 5/3 rational surface shifts inward by 0.0364 for case 1 and 0.0725 for case 2, and shifts outward by 0.0669 for case 3 (case 1 and 3 not shown in figure 1).

The time evolution of the volume integral of the density, $\int_0^a r\,\langle n_e(r)\rangle\,dr$, for the cases considered is plotted in figure 2 (left). The density is normalized to the equilibrium value at the axis n_{e0}, r is normalized to a, and times are normalized to the resistive time, τ_R. The density source that simulates the pellet is added at $t = 0.16\tau_R$ for a time interval of $0.002\tau_R$. One can see that: there is a clear decrease in confinement when the 5/3 rational surface is out of the plasma (case 3a); the best confinement is when the 5/3 rational surface is located at the density gradient (cases 1a, 2a and 4); the confinement does not improve when the entire ι-profile is shifted and the 8/5 rational surface is not in the plasma (cases 1b and 2b).

In Figure 2 (right), we show the resulting simulated density profiles, before and after the application of the density pulse, as well as the profiles of the different cases considered (averaged

Figure 2: Left: time evolution of the volume integral of the density. Right: Density profiles before and after applying the density pulse, and time-averaged profiles of the different cases.

over time after pellet injection). Again, it is clear that the confinement improves as the $5/3$ rational surface penetrates the plasma, as long as the $8/5$ rational surface is inside the plasma, or when the rotational transform profile has a double rational surface $5/3$ well inside the plasma.

The increase of the plasma density in the model causes an increase of the density gradient. This enhanced gradient triggers the growth of interchange instabilities, mainly at the position of low order resonant surfaces. Once these modes are activated, associated local shear flows develop that affect the turbulent particle flux $\Gamma = \left\langle \tilde{V}_r \tilde{n}_e \right\rangle$. The local maxima of the particle flux are mainly linked to the low-order rational surfaces. Figure 3 shows the radial profiles (averaged over time) of the particle flux for the standard case (currentless) and for case 4, where a clear decrease in the flux is observed for case 4. The same happens in cases 1a and 2a, while the flux increases in case 3a, and changes slightly in cases 1b and 2b.

Figure 3: Radial particle flux profile of standard case and case 4. The locations of some low order rational surfaces n/m are indicated.

To quantify the improvement of turbulent transport, we define an effective particle confinement time, τ_{eff}, as $\tau_{eff}(r) = \int_0^r x \langle n_e(x) \rangle \, dx / (r\Gamma(r))$.

Through a radial average of the effective confinement time, we can calculate the temporal evolution of the effective turbulence particle confinement time. Figure 4 (left) shows the evo-